Method for measuring the steering wheel angle of paddy field agricultural machinery by integrating RTK-GNSS and dual-MEMS gyroscope

Pei Wang[1,2,3,4], Lian Hu[1,2,3,4], Jie He[1,2,3,4*], Siqi Ke[2], Zhongxian Man[1,2,3], Tuanpeng Tu[1,2,3], Luning Yang[1,2,3], Yuanyuan Li[1,2,3], Yanling Yi[1,2,3], Weicong Li[1,2,3], Xiwen Luo[1,2,3]

(1. *College of Engineering, South China Agricultural University, Guangzhou 510642, China;*
2. *Key Laboratory of Key Technology on Agricultural Machine and Equipment, Ministry of Education, South China Agricultural University, Guangzhou 510642, China*; 3. *Guangdong Provincial Key Laboratory for Agricultural Artificial Intelligence (GDKL-AAI), Guangzhou 510642, China*; 4. *Maoming Branch, Guangdong Laboratory for Lingnan Modern Agriculture, Maoming 525000, Guangdong, China*)

Abstract: Aiming at the application environment of paddy agricultural machinery with bumpy and undulating changes, the problems affecting the method for steering wheel angle measurement by MEMS gyroscope were analyzed, and a wheel angle measurement method combining Dual-MEMS gyroscope (dual MEMS gyroscope) and RTK-GNSS was designed. The adaptive weighting method was used to fuse the heading angle differentiation of RTK-GNSS, the MEMS gyroscope angle rate, and velocity data, and the rod-arm compensation was performed to accurately obtain the angle rates of the body and steering wheels of agricultural machinery; the difference between the combined angular rate of the steering wheel of the agricultural machinery and the angular rate of the agricultural machinery body was obtained, and the integrator is used to integrate the difference to get the wheel steering angle value, and the Kalman filter was designed to make feedback correction for the integration process of angle calculation to eliminate the errors caused by the gyroscope zero bias, random drift, and gyroscope rod arm effect, and to obtain the accurate value of wheel steering angle. A comparative test with the connecting rod wheel angle sensor was designed, and the results show that the maximum deviation is 4.99 °, the average absolute average value is 1.61 °, and the average standard deviation is 0.98 °. The method in this study and the connecting rod wheel angle sensor were used on paddy farm machinery. The wheel angle measurement deviation of the proposed method and the connecting rod wheel angle sensor was not more than 1 °, which is relatively small. It has good stability, speed adaptability, and dynamic responsiveness that meets the accuracy requirements of steering wheel angle measurement for paddy field agricultural machinery unmanned driving and can be used instead of connecting rod angle sensors for unmanned agricultural machinery.
Keywords: steering wheel angle, MEMS gyroscope, Kalman filter, agricultural machinery navigation, agricultural machinery
DOI: 10.25165/j.ijabe.20221506.7523

Citation: Wang P, Hu L, He J, Ke S Q, Man Z X, Tu T P, et al. Method for measuring the steering wheel angle of paddy field agricultural machinery by integrating RTK-GNSS and dual-MEMS gyroscope. Int J Agric & Biol Eng, 2022; 15(6): 197–205.

1 Introduction

The steering angle of the front wheels is important information for the movement of unmanned agricultural machinery[1]. The front wheel steering angle measurement is one of the key technologies of agricultural machinery automatic navigation[2,3]. The only control variable of the unmanned wheeled agricultural machine is the steering angle of the front wheels[4,5]. Therefore, the accurate measurement of the steering angle is very important[6]. The steering of wheeled agricultural machinery is achieved by driving the front wheel of the vehicle to deflect an angle relative to the body. In order to accurately measure the steering wheel angle of agricultural machinery, the optimal solution is to carry out the overall design of the agricultural machinery when it leaves the factory, but the current agricultural machinery still lacks the unmanned design of the whole machine[7]. Therefore, in order to obtain the steering angle of the unmanned agricultural machine, the most direct way is to install a link-type sensor on the steering wheel[8-10] and use a flexible coupling to connect it with the wheel shaft[11]. But in practice, the main problems in the application are as follows: 1) the sensor is difficult to install, and the vehicle adaptability is poor; 2) the zero position of the wheel angle is easy to change, and recalibration is time-consuming and labor-intensive; 3) the connecting rod easily loosens or breaks. Therefore, domestic and foreign scholars have proposed a non-contact wheel angle measurement method[12-16]. Install an inertial sensor on the front wheel shaft of agricultural machinery to measure the steering angle speed of the front wheels, and then obtain the steering wheel angle; using inertial devices such as a gyroscope installed in the steering wheel to indirectly measure the steering angle of the agricultural machinery front wheels through the steering

Received date: 2022-03-17 **Accepted date:** 2022-10-30
Biographies: Pei Wang, PhD, Lecturer, research interest: intelligent agricultural machinery, Email: wangpei@scau.edu.cn; **Lian Hu**, PhD, Professor, research interest: intelligent agricultural machinery and unmanned farm, Email: lianhu@scau.edu.cn; **Siqi Ke**, Master candidate, research interest: intelligent control, Email: ke000024@umn.edu; **Zhongxian Man**, Mater candidate, research interest: unmanned farm research, Email: 371270285@qq.com; **Tuanpeng Tu**, PhD candidate, research interest: intelligent control of agricultural machinery, Email: 1024462631@qq.com; **Luning Yang**, Master candidate, research interest: high precision map, Email: 971544588@qq.com; **Yuanyuan Li**, Master candidate, research interest: path planning, Email: 775482645@qq.com; **Yanling Yi**, Master candidate, research interest: precision operation control, Email: 1173420175@qq.com; **Weicong Li**, Mater candidate, research interest: obstacle avoidance system, Email: 837801105@qq.com; **Xiwen Luo**, Master, Professor, research interest: smart agriculture, Email: xwluo@scau.edu.cn.

***Corresponding author: Jie He**, PhD, Experiment technician, research interest: agricultural machinery navigation. Agricultural Engineering Building, South China Agricultural University, No. 483, Wushan Road, Tianhe District, Guangzhou 510642, China. Tel.: +86-20-38676975, Email: hooget@scau.edu.cn.

transmission relationship allows easier installation and wiring than other methods. The method is simple but exhibits poor adaptability to agricultural machinery steering system performance, steering clearance, etc.[17] Huang et al.[18] installed sensors such as encoders and inertial devices in a steering wheel to establish the relationship between the steering wheel and the steering angle of the front wheels to detect the steering angle. Miao et al.[19] proposed a dual-antenna GNSS and MEMS gyroscope. For the rotation angle measurement system, the error between the measured wheel steering angle measured by a test and the output result of the absolute angle sensor was within 0.5 °, and the error was within 1 ° during a curve test. Miao et al.[20] adopted GNSS fusion with MEMS Gyro and introduced gyroscope lever arm effect compensation to measure the rotation angle of the front wheel of the tractor, and obtained high measurement accuracy. Using a low-cost micro-electromechanical system (MEMS) combined with GPS and unscented Kalman filter (UKF) to estimate the steering angle of agricultural vehicles, a better wheel angle measurement accuracy was obtained[21]. The dual-antenna combined with the MEMS gyroscope's steering angle measurement scheme reduces the system cost, but due to the low update rate of the dual-antenna GNSS heading, the measurement accuracy is not high[22,23], which affects the accuracy of the measurement system, and the accelerometer's installation position is difficult to match with the swing reference point of the carrier. In an angular motion environment, the output of the accelerometer produces interference acceleration relative to the reference point, which is affected by the lever arm effect[24-28], which also affects the measurement accuracy.

In summary, this study proposed an improved dual-MEMS gyroscope (dual gyroscope) and RTK-GNSS fusion wheel angle measurement method for the bumpy and undulating application environment of paddy field agricultural machinery to eliminate gyroscope bias and randomness. Errors caused by drift, as well as errors caused by the arm effect of the gyroscope, improve the usability and accuracy of wheel angle measurement.

2 Materials and methods

2.1 Principle of steering wheel angle measurement

A schematic diagram of the steering wheel angle measurement principle is shown in Figure 1. MEMS1 is a gyroscope mounted on the body of the farm machine to measure the combined angular rate $\dot{\theta}+\dot{\phi}$ of the farm machine steering wheels, where $\dot{\phi}$ is the body angular rate obtained by fusing $\dot{\phi}_1$ and $\dot{\phi}_2$, $\dot{\phi}_1$ and $\dot{\phi}_2$ is the farm machine body angular rate measured by the MEMS2 mounted on the front wheel steering column of the farm machine and RTK-GNSS mounted on the farm machine body, respectively, and $\dot{\theta}$ is the measured pure steering angular rate. In order to accurately obtain the angular rates of the farm machinery body and steering wheels, the angular rates and velocities measured by MEMS gyroscope and RTK-GNSS need to be compensated by the lever arm; to meet the needs of steering wheel angle measurement during low-speed start-up and high-speed operation of agricultural machinery, MEMS1 and RTK-GNSS were used to measure the steering rate $\dot{\phi}_1$ and $\dot{\phi}_2$ of agricultural machinery body, respectively, and data fusion processing was performed; to get the pure steering wheel rate $\dot{\theta}$ by making a difference between the obtained combined angular rate $\dot{\theta}+\dot{\phi}$ of the steering wheels of the agricultural machine and the angular rate $\dot{\phi}$ of the body of the agricultural machine, and to get the calculated value θ of the wheel steering angle by integrating the pure steering wheel rate $\dot{\theta}$ using an integrator. The result of the difference between the calculated and observed values $\arctan(\dot{\phi}L/v)$ is substituted into the Kalman filter as the measured value for optimal estimation, and the angular error of the Kalman filter output and the gyro zero bias performs feedback correction on the angle calculation integration process to calculate accurate information of the wheel turning angle θ. In order to eliminate the system error due to Ackermann steering nonlinearity of the left and right front wheels of the agricultural machine installed in the MEMS2 gyroscope, Ackermann nonlinearity compensation is designed and used to acquire the center steering wheel angle θ_c of the agricultural machine.

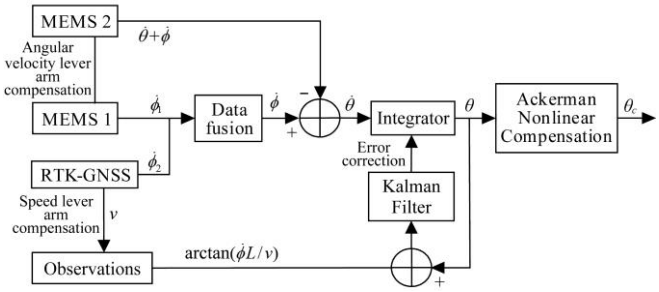

Note: $\dot{\theta}$ is the pure steering wheel rate; $\dot{\phi}$ is the angular rate; $\dot{\theta}+\dot{\phi}$ is the obtained combined angular rate; θ_c is the center steering wheel angle; $\arctan(\dot{\phi}L/v)$ is the calculated and observed values; $\dot{\phi}_1$ and $\dot{\phi}_2$ are the steering rate.

Figure 1 Principle of steering wheel angle measurement

2.1.1 Observation estimate

Wheeled agricultural machinery often adopts the two-wheeled Ackerman steering model[29,30]. The kinematics equation of agricultural machinery in the Gaussian plane rectangular coordinate system is

$$\begin{aligned}\dot{x} &= v\cos(\phi)\\ \dot{y} &= v\sin(\phi)\\ \dot{\phi} &= v\tan(\theta)/L\end{aligned} \tag{1}$$

where, θ is the steering angle of the front wheels, (°); ϕ is the angular rate of the agricultural machinery body, rad/s; v is the agricultural machinery body speed, m/s; R is the tractor turning radius, m; L is the tractor wheelbase, m.

From Equation (1), the calculation equation of the steering wheel angle is

$$\alpha = \arctan(\dot{\phi}L/v) \tag{2}$$

Equation (2) can be used as an observation value for the optimal estimation of the steering angle of the front wheels.

2.1.2 RTK-GNSS heading angle rate filtering

The heading output frequency of the RTK-GNSS board is 10 Hz, and the heading angular rate obtained by the direct differential processing of the heading is noisy. In this paper, an adaptive Kalman filter is designed to filter the heading angular rate by continuously changing the model parameters or noise statistical characteristics. Real-time estimation and correction can realize the online improvement of the filter, reduce the actual filtering error, and improve the dynamic performance of the Kalman filter. This method can effectively integrate system identification and filtering estimation[31].

Assuming that the angular acceleration of the vehicle body is 0 when the agricultural machinery is driving in a straight line and there is a normal distribution of random noise, Kalman filtering can be performed on the heading angular rate in the straight-line

navigation state as follows:

$$\dot{\phi}_k = \dot{\phi}_{k-1} + a\Delta t + w_g \tag{3}$$

where, $\dot{\phi}_k$ is the angular rate of the agricultural machinery body at the current moment; $\dot{\phi}_{k-1}$ is the angular rate of the agricultural machinery body at the previous moment, a=0, and w_g is Gaussian white noise.

The state variable of the Kalman filter is the angular rate of the agricultural machinery body. There is no control input, so the state transition matrix $\boldsymbol{A}$=1; the observation value containing the noise is the direct manifestation of the state variable, so the measurement matrix $\boldsymbol{H}$=1. The state equation and observation equation of the Kalman filter were established as shown in Equations (3) and (4).

Equation of state:

$$X_k = AX_{k-1} + w_g \tag{4}$$

Observation equation:

$$Z_k = HX_k + v_g \tag{5}$$

where, X_k is the angular rate of the agricultural machine body at time k; X_{k-1} is the angular rate of the agricultural machine body at time k+1; Z_k is the observed value of the body rotation rate after dual GNSS heading differentiation at time k; v_g is the Gaussian white noise.

According to the filter iteration principle, the Kalman filter time update equations as Equations (6) and (7) and the measurement update equations (Equations (8)-(10)) were established.

$$\hat{x}_k^- = \hat{x}_{k-1} \tag{6}$$

$$P_k^- = P_{k-1} + Q \tag{7}$$

$$K_k = P_k^- / (P_k^- + R) \tag{8}$$

$$\hat{x}_k = \hat{x}_k^- + K_k(Z_k - \hat{x}_k^-) \tag{9}$$

$$P_k = (I - K_k)P_k^- \tag{10}$$

where, $\hat{x}_{k-1}$ is the a priori state estimate at time k−1; $\hat{x}_k^-$ is the a posteriori state estimate at time k; P_k^- is the estimated covariance of the a priori state estimate at time k; P_{k-1} is the estimated covariance of the a posteriori state estimate at time k−1; Q is the covariance matrix of the procedure activation noise; K_k is the Kalman gain; R is the covariance matrix of the observation noise; $\hat{x}_k$ is the a posteriori state estimate at time k; $\hat{x}_k^-$ is the a priori state estimate at time k.

Since the angular acceleration of the vehicle body cannot be approximated as 0 when the agricultural machinery is traveling on a curve, the Kalman filter model is mismatched when the agricultural machinery is traveling on a curve. This study proposed a process excitation noise covariance matrix $\boldsymbol{Q}$ based on the agricultural machinery transverse tracking deviation to adaptively adjust the Kalman filter. When the Kalman filter determines that the agricultural machinery is in the online process, the weight value of the Kalman filter can be changed by increasing the Q value. Then the problem of model mismatch is solved.

$$Q = \begin{cases} \dfrac{|pe_{now}|}{|pe_{\max}| - |pe_{\min}|}(q_{\max} - q_{\min}) + q_{\min} & (0.1 < |pe_{now}| < 3) \\ q_{\min} & (|pe_{now}| < 0.1) \end{cases} \tag{11}$$

where, pe_{now} is the lateral tracking deviation of the current agricultural machinery; $pe_{\max}$ and $pe_{\min}$ are the maximum online distance and the minimum online distance, respectively; $q_{\max}$ and $q_{\min}$ are the maximum and minimum values of the adaptive Kalman filter process excitation noise covariance matrix $\boldsymbol{Q}$ initialization, respectively.

2.1.3 Lever arm effect compensation

Generally, when the wheel angle measurement system is actually installed, it is difficult for the RTK-GNSS antenna and MEMS1 to coincide with the center of mass of the agricultural machinery. As shown in Figure 2, this introduces a systematic measurement error[32,33].

In this study, the lever arm of the vehicle body speed v and the car body angular rate $\dot{\phi}_2$ measured by RTK-GNSS were needed to compensate; compensate the lever arm effect of the $\dot{\phi}_1$ measured by the MEMS1 gyroscope; performed the lever arm effect compensation on the vehicle body measured by the MEMS2 gyroscope. The angular velocity $\dot{\phi}$ was used for lever arm compensation; the MEMS2 gyroscope was installed near the center of the front wheel steering column, the lever arm effect of the pure steering angle rate $\dot{\theta}$ was not significant, and the lever arm effect was ignored in this study.

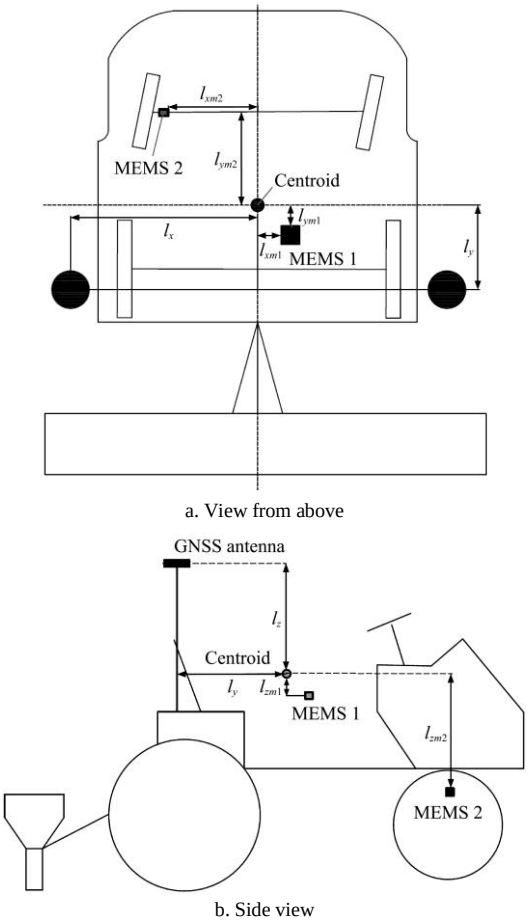

Note: l_x, l_y, and l_z are the distances from the GNSS antenna to the center of agricultural machinery respectively; l_{xm1}, l_{ym1}, and l_{zm1} are the distances from the MEMS1 to the center of agricultural machinery respectively, l_{xm2}, l_{ym2}, and l_{zm2} are the distances from the MEMS2 to the center of agricultural machinery respectively.

Figure 2 Schematic diagram of GNSS and MEMS lever arm

As shown in Figure 3, we define the coordinate system b of the agricultural machinery carrier with the center of mass as the origin. The x-axis points to the right along the horizontal axis of the carrier, the y-axis points forwards along the vertical axis of the carrier, and the z-axis points upwards along the vertical axis of the carrier. Then, the coordinate conversion matrix from the carrier coordinate system b to the navigation coordinate system t (Northeast Sky

Geographical Coordinate System) is

$$R_b^t=\begin{bmatrix}\cos\gamma\cos\varphi-\sin\gamma\sin\varphi & -\sin\varphi & \sin\gamma\cos\varphi+\cos\gamma\sin\varphi\\ \cos\gamma\sin\varphi+\sin\gamma\cos\varphi & \cos\varphi & \sin\gamma\sin\varphi-\cos\gamma\cos\varphi\\ -\sin\gamma & 0 & \cos\gamma\end{bmatrix} \quad (12)$$

where, φ and γ are respectively the heading angle and roll angle of agricultural machinery obtained by RTK-GNSS.

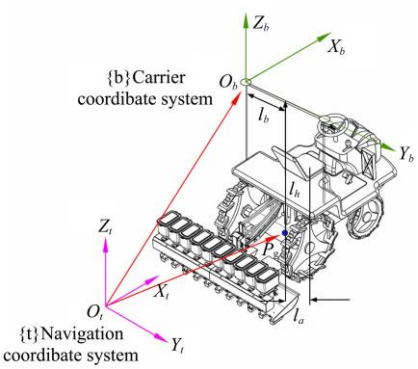

Note: $O_bX_bY_bZ_b$ represents the carrier coordinate system; $O_tX_tY_tZ_t$ indicates the navigation coordinate system; l_a and l_b are the distances of the main positioning antenna from the implement suspension point and the center of the vehicle, respectively, and l_h is the difference in the elevation between the main positioning antenna and the implement suspension point.

Figure 3 Agricultural machinery carrier and navigation coordinate system

The lever arm length vector of the RTK-GNSS antenna and the centroid of the agricultural machinery is

$$l_{gnss}=[l_x \quad l_y \quad l_z]^{\mathrm{T}} \quad (13)$$

The rotation angular rate vector of the agricultural machinery is

$$\omega_{tb}^b=[0 \quad \dot{\gamma} \quad \dot{\varphi}]^{\mathrm{T}} \quad (14)$$

The rotation angular acceleration vector of the agricultural machinery is

$$a_{tb}^b=[0 \quad \ddot{\gamma} \quad \ddot{\varphi}]^{\mathrm{T}} \quad (15)$$

The speed error due to the lever arm effect is

$$e_v=\begin{bmatrix}e_{vx}\\ e_{vy}\\ e_{vz}\end{bmatrix}=R_b^t(\omega_{tb}^b\times l_{gnss}) \quad (16)$$

The error of the vehicle body angular rate $\dot{\phi}_2$ due to the lever arm effect is

$$e_{\dot{\phi}_2}=\begin{bmatrix}e_{\dot{\phi}_2x}\\ e_{\dot{\phi}_2y}\\ e_{\dot{\phi}_2z}\end{bmatrix}=R_b^t(a_{tb}^b\times l_{gnss}) \quad (17)$$

The horizontal velocity v_{gnss} measured by RTK-GNSS is decomposed into the true east and true north directions along the heading angle of the agricultural machinery movement.

$$v_{gnss}=[v\cos\varphi \quad v\sin\varphi \quad 0]^{\mathrm{T}} \quad (18)$$

The vehicle body angular rate $\dot{\phi}_{2gnss}$ measured by RTK-GNSS is decomposed into the true east and true north directions along the direction of the agricultural machinery movement heading angle.

$$\dot{\phi}_{2gnss}=[\dot{\phi}_2\cos\varphi \quad \dot{\phi}_2\sin\varphi \quad 0]^{\mathrm{T}} \quad (19)$$

The speed v after lever arm compensation is

$$v=[v_x \quad v_y \quad 0]^{\mathrm{T}}=v_{gnss}-e_v \quad (20)$$

The angular rate of the vehicle body measured by RTK-GNSS after lever arm compensation is

$$\dot{\phi}_2=[\dot{\phi}_{2x} \quad \dot{\phi}_{2y} \quad 0]^{\mathrm{T}}=\dot{\phi}_{2gnss}-e_{\dot{\phi}_2} \quad (21)$$

The agricultural machinery body is regarded as a rigid body. The heading angle and roll angle of MEMS1 and MEMS2 can be respectively expressed by φ and γ measured by RTK-GNSS, and the coordinate conversion matrix from the carrier coordinate system b to the navigation coordinate system t is also R_b^t.

The lever arm length vector of the MEMS1 gyroscope and the centre of mass of the agricultural machinery body is

$$l_{mems1}=[l_{xm1} \quad l_{ym1} \quad l_{zm1}]^{\mathrm{T}} \quad (22)$$

The lever arm length vector of the MEMS2 gyroscope and the centroid of agricultural machinery is

$$l_{mems2}=[l_{xm2} \quad l_{ym2} \quad l_{zm2}]^{\mathrm{T}} \quad (23)$$

The angular accelerations measured by the MEMS1 and MEMS2 gyroscopes rotating around the z-axis are a_{1tb}^b and a_{2tb}^b, respectively.

$$a_{1tb}^b=[a_{1x} \quad a_{1y} \quad a_{1z}]^{\mathrm{T}} \quad (24)$$

$$a_{2tb}^b=[a_{2x} \quad a_{2y} \quad a_{2z}]^{\mathrm{T}} \quad (25)$$

The body angular rate error due to the lever arm effect of MEMS1 is

$$e_{\dot{\phi}_1}=\begin{bmatrix}e_{\dot{\phi}_1x}\\ e_{\dot{\phi}_1y}\\ e_{\dot{\phi}_1z}\end{bmatrix}=R_b^t(a_{1tb}^b\times l_{mems1}) \quad (26)$$

The body angular rate $\dot{\phi}$ error due to the MEMS2 lever arm effect is

$$e_{\dot{\phi}}=\begin{bmatrix}e_{\dot{\phi}x}\\ e_{\dot{\phi}y}\\ e_{\dot{\phi}z}\end{bmatrix}=R_b^t(a_{2tb}^b\times l_{mems2}) \quad (27)$$

The angular velocity of the vehicle body measured by MEMS1 is decomposed into the true east and true north directions along the direction of the agricultural machinery movement heading angle.

$$\dot{\phi}_{mems1}=[\dot{\phi}_1\cos\varphi \quad \dot{\phi}_1\sin\varphi \quad 0]^{\mathrm{T}} \quad (28)$$

The angular velocity of the vehicle body measured by MEMS1 is decomposed into the true east and true north directions along the direction of the agricultural machinery movement heading angle.

$$\dot{\phi}_{mems2}=[\dot{\phi}\cos\varphi \quad \dot{\phi}\sin\varphi \quad 0]^{\mathrm{T}} \quad (29)$$

The angular velocity $\dot{\phi}_1$ measured by MEMS1 after lever arm compensation is

$$\dot{\phi}_1=[\dot{\phi}_{1x} \quad \dot{\phi}_{1y} \quad 0]^{\mathrm{T}}=\dot{\phi}_{mems1}-e_{\dot{\phi}_1} \quad (30)$$

The body angular rate $\dot{\phi}$ measured by MEMS2 after lever arm compensation is

$$\dot{\phi}=[\dot{\phi}_x \quad \dot{\phi}_y \quad 0]^{\mathrm{T}}=\dot{\phi}_{mems2}-e_{\dot{\phi}} \quad (31)$$

2.1.4 Weighted data fusion

It can be seen from the literature[34,35] that the GNSS heading differential can be adapted to the measurement of the steering wheel angle of agricultural machinery at lower speeds; the noise is greater when operating at higher speeds, and the stability of the front-wheel steering angle measurement system is worse. With dual MEMS gyroscopes, the measurement frequency is high, but because the MEMS gyroscope needs a certain period of time to obtain stable operation to provide a better wheel angle measurement output, the wheel angle output is momentarily inaccurate when the agricultural machine stops and restarts. To integrate the advantages of GNSS heading differentiation and MEMS angular velocity measurement, this paper uses the method of adaptive weighted fusion of GNSS and MEMS to obtain the angular velocity of the agricultural vehicle body.

$$\dot{\phi}=\sum_{i=1}^{n}\left(W_{1i}\cdot\dot{\phi}_{1i}+W_{2i}\dot{\phi}_{2i}\right) \tag{32}$$

$$\sum_{i=1}^{n}\left(W_{1i}+W_{2i}\right)=1 \tag{33}$$

where, $\dot{\phi}_{1i}$ and $\dot{\phi}_{2i}$ are the i-th measured values of MEMS1 and RTK-GNSS, respectively; W_{1i} and W_{2i} are the weights of $\dot{\phi}_{1i}$ and $\dot{\phi}_{2i}$, respectively.

To increase the contribution of the GNSS heading differential to agricultural machinery steering wheel angle measurement at low speeds, based on the agricultural machinery speed design weights W_{1i} and W_{2i}, the min-max normalization method is used to compensate the speed v_i at the i-th moment and return one value:

$$v_{Ni}=\frac{v_i}{v_{\max}} \tag{34}$$

where, $v_{\max}$ is the highest speed of agricultural machinery operation; v_{Ni} is the normalized standard value.

$$\begin{cases}W_{1i}=1-1/v_{Ni} & (v_{Ni}\neq 0)\\ W_{1i}=1 & (v_{Ni}=0)\end{cases} \tag{35}$$

$$\begin{cases}W_{2i}=1/v_{Ni} & (v_{Ni}\neq 0)\\ W_{2i}=0 & (v_{Ni}=0)\end{cases} \tag{36}$$

2.1.5 Kalman filter design

During the driving process of paddy farm machinery, a change in the front wheel angle causes a change in the body head. The resultant rate measured by the gyro on the front wheel steering axis of the vehicle includes the rotation rate of the wheel relative to the body and the rotation rate of the wheel.

$$\omega=\dot{\theta}+\dot{\phi} \tag{37}$$

where, the gyro MEMS2 measures the combined rate of wheel rotation. The transformation equation can be obtained

$$\dot{\theta}=\omega-\dot{\phi} \tag{38}$$

Equation (38) integrates the time to obtain the steering wheel angle of the wheels:

$$\theta=\int(\omega-\dot{\phi})dt \tag{39}$$

However, because the output of the MEMS gyroscope has error items such as random drift and zero offset, denoted as ξ, the integral calculation of the steering wheel angle of Equation (39) introduced error in the gyro results, and the accumulation of time caused the measured value of the steering wheel to diverge. The angle feedback for navigation control was used in this study. Introducing the gyro error term, the true steering wheel angle is

$$\theta_t=\int(\omega-\xi-\dot{\phi})dt \tag{40}$$

Derivation of both sides of Equation (40) yields

$$\dot{\theta}_t=\omega-\xi-\dot{\phi} \tag{41}$$

Noise is usually present:

$$\dot{\theta}_t=\omega-\xi-\dot{\phi}+w_g+w_\varphi \tag{42}$$

where, w_g represents the Gaussian white noise measured by the front wheel shaft gyro; w_φ represents the Gaussian white noise measured by the body rotation rate.

The measured value of the steering wheel angle is shown in Equation (2), and the measured value is composed of the real angle value θ_t and the measured Gaussian white noise w_a.

$$\alpha=\theta_t+w_a \tag{43}$$

Assuming that the measurement noise and the estimated noise are independent of each other, the observation value is used to estimate the zero deviation of the wheel steering axis gyro integral measurement angle to construct the discrete Kalman filter state equation and observation equation, as shown in Equations (43) and (44), respectively.

$$X'_k=\begin{bmatrix}1 & -\Delta t\\ 0 & 1\end{bmatrix}X'_{k-1}+\begin{bmatrix}\Delta t\\ 0\end{bmatrix}\left[\omega_k-\dot{\phi}_k\right]+\begin{bmatrix}w_g+w_\varphi\\ w_v\end{bmatrix} \tag{44}$$

$$Z'_k=\begin{bmatrix}1 & 0\end{bmatrix}X'_k+w_a \tag{45}$$

where, X'_k represents the state variable at time k; X'_{k-1} represents the state variable at time k+1; Δt represents the Kalman filter calculation update frequency; ω_k represents the wheel rotation rate output by the MEMS2 gyro at time k; $\dot{\phi}_k$ represents the body rotation rate output by MEMS1 at time k; Z'_k represents the observed value of the front wheel angle calculated by the heading angular rate of the tractor body and the center speed of the rear wheel axle at that moment; w_v and w_a both refers to Gaussian white noise.

The time update estimation and measurement update calibration equations of the Kalman filter were established as Equations (6)-(10), iteratively solve the front wheel steering angle and gyro bias estimation problems, and obtain the optimal estimated steering angle value θ_c of the covariance.

2.1.6 Ackerman steering nonlinear compensation

The above-mentioned steering wheel angle measurement method treats agricultural machinery as a two-wheeled vehicle model. The steering angle θ_c is the virtual wheel steering wheel angle at the center of the agricultural machinery's front axle. The actual sensor may be installed on the left or right front wheel, and θ_c represents steering with the left and right front wheels. The geometric relationship of the angles is shown in Figure 4.

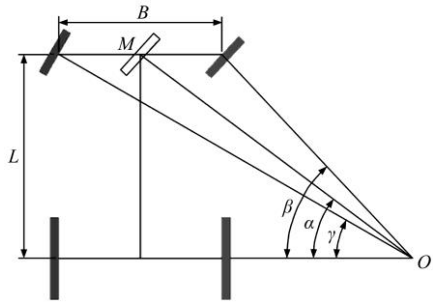

Note: B is the wheelbase of the front wheel; L is the center distance of the front and rear wheels; M is the center of the virtual wheel; β, α, γ are the Angle between the steering origin and the right front wheel, the virtual wheel center, and the left front wheel, respectively.

Figure 4 Geometric relationship between virtual wheel angle and actual wheel angle

From Figure 4, the relationship between the virtual wheel steering angle and the real left and right front wheel steering angles of the two-wheeled vehicle model is given in Equations (46) and (47), respectively.

$$\cot\gamma=\cot\alpha+B/(2L) \tag{46}$$

$$\cot\beta=\cot\alpha+B/L \tag{47}$$

where, γ and β respectively represent the steering angle of the left and right front wheels of the agricultural machinery.

2.2 Experiment material

The Shanghai Star rice direct-bearing model (with Yanmar YR60D head) was used as the research platform, and the linkage wheel angle sensor was used as the contrast steering wheel angle measurement sensor. Among the components, the connecting rod type angle sensor adopts BEI's DUNCAN9360 model angle sensor (12-bit Hall-type position sensor, with a resolution of 2160 ° and a

linearity of ±0.5%). The installation is shown in Figure 5. The installation of wheel angle sensor include 11 parts. Among them, the socket inner cleats are fixed to the wheel steering arm by fixing bolts, the lever of the paddle seat was socketed in the guide groove of the guide groove follower arm, the guide groove was hinged to the end of the follower arm on the hinge base, the hinge base was fixed to the frame, the sensor fixing plate was placed between the hinge base and the frame through bolts, the angle sensor was fixed to the sensor fixing plate, one section of the extension arm was fixed to the angle sensor rotating shaft, one section was fixed to one end of the double ball head rod, and the other end of the double ball head rod was fixed to the guide groove slave arm.

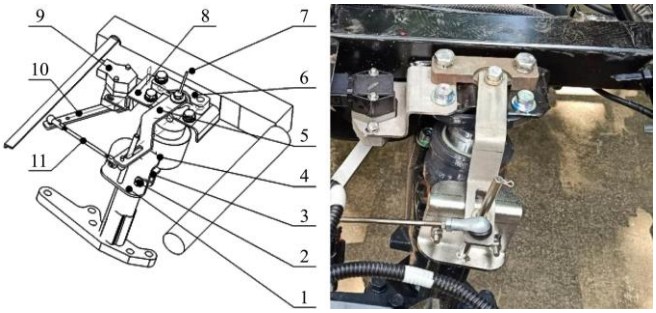

a. Wheel Angle sensor installation structure drawing b. Wheel Angle sensor installation picture

1. Socket inner splint 2. Fixing bolt 3. Wheel steering arm 4. Paddle seat 5. Guide groove follower arm 6. Hinged base 7. Frame 8. Sensor fastening plate 9. Angle sensor 10. Extension arm 11. Double ball head rod

Figure 5 Installation drawing of angle sensor for rice transplanter/rice direct seeding machine

The heading and attitude reference system (AHRS) uses the MTi-300 inertial sensor produced by XSENS Technologies in the Netherlands, as shown in Figure 6c, which can measure the attitude (roll angle, pitch angle and heading angle) and acceleration of the rice transplanter body and provides angular velocity information. The static attitude measurement accuracy of MTi-300AHRS corresponds to the dynamic measurement accuracy. During the test, the update frequency of the AHRS is set to 50 Hz.

a. YR60 rice seeding machine

b. Sinan K726OEM board

c. MTi-300 AHRS

d. 3-axis gyroscope

Figure 6 Test platform and main sensers

The dual gyroscope sensor includes a three-axis gyroscope and a single-axis gyroscope using two LINS300 MEMS gyroscopes from Wuxi Lingsi Technology Co., Ltd., China, which are set for three-axis and single-axis use, respectively, as shown in Figure 6d.

The positioning system on the direct seeding machine adopts the K726 Beidou dual antenna satellite positioning OEM board produced by Shanghai Sinan Satellite Navigation Technology Co., Ltd., China, as shown in Figure 6b. The K726 positioning data output frequency is 20 Hz, the data interface is RS232, the RTK horizontal positioning accuracy is 1 mm+1 parts per million (ppm), and the RTK heading angle accuracy is. During the test, the K726 OEM board is integrated into the driverless main controller.

2.3 Experiment method

To obtain an accurate measurement method for measuring the steering wheel angle of paddy field agricultural machinery, the linkage wheel angle measurement method was compared with the MEMS measurement method described in this study. Therefore, the design experiment was designed to test the linkage wheel angle measurement and the dual MEMS fusion GNSS heading differential method path. The measurement accuracy and dynamic response characteristics were tested and compared.

The test installation and related parameters are designed as follows:

1) The DUNCAN9360-type angle sensor is installed with the front wheel axle centre link type, the heading is provided by the Sinan K726 dual antennas, and two LINS300 MEMS gyroscope measuring devices are installed under the front wheel steering column and the front centre seat.

2) The Kalman filter initialization parameters are $P(0)=\begin{bmatrix}100 & 0\\ 0 & 100\end{bmatrix}$, $Q(0)=\begin{bmatrix}0.01 & \\ & 0.01\end{bmatrix}$, and R=0.5. The initialization parameters of the adaptive Kalman filter are P(0)=100 and Q(0)=0.005. These parameters are selected based on trial and experience. The adaptive formula of Q is

$$Q(pe)=\begin{cases}(|pe|-0.1)/2.9*0.295+0.005 & 0.1<|pe|<3\\ 0.005 & |pe|<0.1\end{cases} \quad (48)$$

The sensor lever arm values are l_{gnss}=[0.8, 0.5, 1.5]^T, l_{mems1}=[0.1, 0.-5, 0.1]^T, and l_{mems2}=[0.5, 1.2, 0.2]^T.

During the test, the unmanned direct seeding machine is equipped with the above-mentioned required sensors, and the linkage wheel angle sensor is used as the input of the wheel angle information of the unmanned driving system. The unmanned driving mode is used to test in the field. The detailed test scheme is as follows: 1) The unmanned direct seeding machine at a velocity of 0.8 m/s along a present path to seed in the paddy field; 2) The seeding operation runs 3 lines of straight lines and 2 steering U-turns. At the same time, the wheel angle information values measured by two-wheel angle measurement methods are obtained for comparison.

3 Test results and analysis

Figure 7 shows a field photograph of the paddy field test, and the wheel angle measurement results are shown in Figure 8. When driving in a straight line, the two-wheel angle measurement methods measure the overall trend of the wheel angles to be consistent, but there are some differences in the details. In Figure 8, when the unmanned direct seeding machine starts, the wheel angle measurement value is stable without notable fluctuations; When measuring the large steering angle, the connecting rod wheel angle measurement method is limited by the nonlinearity of the mechanical structure, and the maximum wheel angle limit can be measured is [−30°, 30°]; the maximum angle of the gyroscope

wheel angle measurement method is affected by the driving speed and heading of the agricultural machine, and the measurement angle range is relatively wide. Therefore, when combining the limit of the steering angle of the paddy field agricultural machine, the gyroscope wheel angle measurement range is set to [−50°, 50°], at approximately 40 s as shown in the figure, the unmanned direct seeding machine starts to perform U-turn steering. The linkage wheel angle sensor responds to steering approximately 0.6 s earlier than the gyroscope, but the gyroscope responds more quickly, and the slope of the large-angle steering response is greater. At the same time, the maximum steering value is reached, indicating that the dynamic response performance of the steering wheel angle measured by the gyroscope is equivalent to the performance of the traditional linkage angle sensor, which can meet the needs of the large steering dynamic response of the paddy farm machinery.

Figure 7 Paddy field test and test site

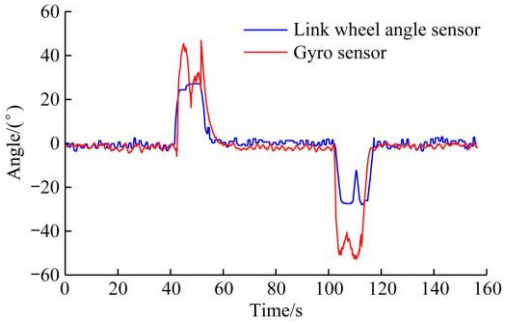

Figure 8 Wheel angle comparison chart

The difference between the wheel angles measured by the two-wheel angle measurement methods is shown in Figure 9. The three-row wheel angle difference of the straight driving part is counted, as shown in Table 1, to investigate the performance of the two-wheel angle measurement methods in a straight line.

From Table 1, it can be seen that the three-line average maximum deviation of the wheel angle measurement of the connecting rod type wheel angle sensor and the gyroscope wheel angle sensor when the agricultural machinery is driving straight is 4.99 °, the average absolute average value is 1.61 °, and the average standard deviation is 0.98 °. The test results show that the gyro wheel angle sensor and the link type wheel angle sensor are used on the paddy field agricultural machinery, and the deviation of wheel angle measurement is not more than 1 °, which is relatively small (based on the link type measurement, and compared with the results of the dryland tractor[23,24]). The system exhibits good stability and meets the accuracy requirements of the unmanned steering wheel angle measurement of the paddy field agricultural machinery, indicating that the gyro wheel angle sensor can replace the connecting rod angle sensor for unmanned agricultural machinery.

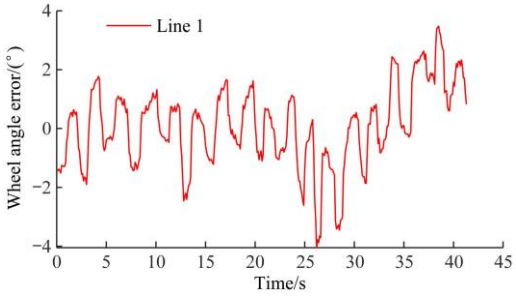

a. The first line Angle measurement difference

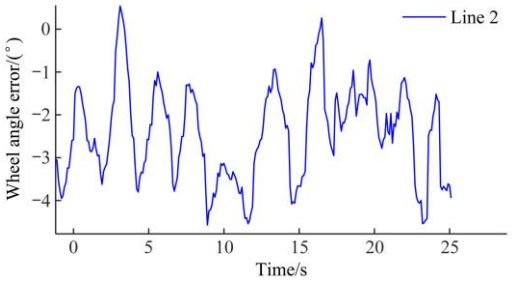

b. The second line Angle measurement difference

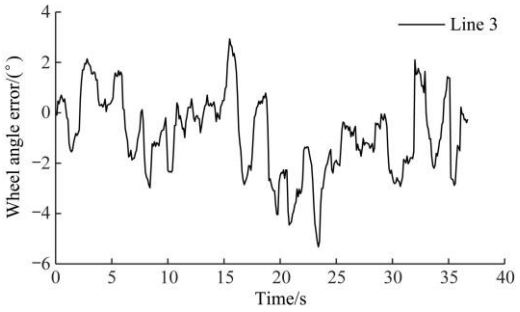

c. The third line Angle measurement difference

Figure 9 Three-line wheel angle difference graph

Table 1 Wheel angle measurement data statistics table (°)

Row	ME	MAE	RMSE
Line 1	3.85	1.01	0.64
Line 2	5.43	2.23	1.04
Line3	5.7	1.58	1.25
Mean	4.99	1.61	0.98

Note: ME: Median; MAE: Mean Absolute Error; RMSE: Root Mean Square Error.

4 Conclusions

This study analyzed the problems that affect the MEMS gyroscope's method of measuring the steering wheel angle in view of the randomly varying application environment of paddy field agricultural machinery. An angle measurement method was developed.

1) MEMS2 installed on the steering column of the front wheels was used to measure the angular rate of the steering wheels and the RTK-GNSS heading angular rate, the MEMS1 gyroscope installed on the body was used to measure the angular rate of the agricultural machinery body, and an adaptive Kalman filter was designed. The device filters the RTK-GNSS heading angular rate and compensates for the angular rate and speed measured by the MEMS gyroscope and RTK-GNSS to accurately obtain the angular rate of the agricultural machinery body and steering wheel.

2) The adaptive weighting method was used for fusion processing of MEMS1 and RTK-GNSS measurements of agricultural machinery body steering rate, combined with the advantages of GNSS heading differential and MEMS gyroscope

angular rate measurement, to solve the problem of inaccurate wheel angle output at the start and stop of paddy farm machinery.

3) A Kalman filter was designed, and the wheel angle information estimated by the kinematics model was used as the observation value. The difference between the steering angle and the observation value obtained by pure steering wheel velocity integration was measured and substituted into the Kalman filter for optimal estimation. The angle error and gyro zero offset output by the Kalman filter were used to feedback and correct the angle calculation and integration process to obtain the precise value of the wheel rotation angle.

4) A comparative test with the connecting rod wheel angle sensor was designed. The results show that the maximum deviation is 4.99 °, the average absolute average value is 1.61 °, and the average standard deviation is 0.98 °. The wheel angle measurement deviation of the proposed method and the connecting rod wheel angle sensor was not more than 1 °, which was relatively small. It has good stability, speed adaptability, and dynamic responsiveness meets the accuracy requirements of steering wheel angle measurement for paddy field agricultural machinery unmanned driving, and can be used instead of connecting rod angle sensors for unmanned agricultural machinery.

5 Discussion

1) Inertial device technology is developing rapidly; the accuracy and stability of MEMS gyroscopes are expected to improve, as will the accuracy and stability of the wheel angle measurement methods described in this study.

2) The weighted design fusion described in this article and the Kalman covariance matrix $\boldsymbol{Q}$ adaptive dynamic adjustment process can use artificial neural network algorithms, genetic algorithms, and other intelligent algorithms to further improve the wheel angle measurement performance of agricultural machinery starting and high-speed driving.

3) When agricultural machinery is operating at higher speeds, such as over 10 km/h, due to the low update frequency of the GNSS board, the noise of the heading differential value is large, and the noise of the MEMS gyroscope when the agricultural machinery moves at high speed in the undulating farmland increases significantly, as described in this article. The accuracy and stability of wheel angle measurement need to be verified.

Acknowledgements

This study was financially supported by Science and Technology Innovation 2030 – “New Generation Artificial Intelligence” Major Project (Grant No. 2021ZD011090202; No. 2021ZD011090503), the National Key Research and Development Program of China (Grant No. 2021YFD2000602), and the National Natural Science Foundation of China (Grant No.32071913; No. 32101623).

[References]

[1] Hu J T, Gao L, Bai X P, Li T C, Liu X G. Review of research on automatic guidance of agricultural vehicles. Transactions of the CSAE, 2015; 31(10): 1–10. (in Chinese)

[2] Ursula K V, Ana S A, Danielle V H, Douglas G, Sophie F, Guillermo J, et al. A review of unmanned vehicles for the detection and monitoring of marine fauna. Marine Pollution Bulletin, 2019; 140: 17–29.

[3] Yin C Q, Wang S R, Li X W, Yuan G, Jiang C. Trajectory tracking based on adaptive sliding mode control for agricultural tractor. IEEE Access, 2020; 8, 113021–113029.

[4] Nguyen Q V. INS/GPS integration system using street return algorithm and compass sensor. Procedia Computer Science, 2017; 103,475–482.

[5] Wang Y X, Li J Q, Wang X, Jin C Q, Yin X. Development and test of a steering angle measuring device for wheeled tractor. Journal of China Agricultural University, 2022; 27(1): 203–211. (in Chinese)

[6] Zhang Z G, Wang G M, Luo X W, He J, Wang J, Wang H. Detection method of steering wheel angle for tractor automatic driving. Transactions of CSAM, 2019; 50(3): 352–357. (in Chinese)

[7] Yin X, Noguchi N. Development and evaluation of a general-purpose electric off-road robot based on agricultural navigation. Int J Agri & Biol Eng, 2014; 7(5): 14–21.

[8] He J, Zhu, J G, Luo X W; Zhang Z G, Hu L, Gao Y. Design of steering control system for rice transplanter equipped with steering wheel-like motor. Transactions of CSAE, 2019; 35(6): 10–17. (in Chinese)

[9] Hu J T, Li T C. Cascaded navigation control for agricultural vehicles tracking straight paths. Int J Agri & Biol Eng, 2014; 7(1): 36–44.

[10] Nagasaka Y, Saito H, Tamaki K, Seki M, Kobayashi K, Taniwaki K. An autonomous rice transplanter guided by global positioning system and inertial measurement unit. Journal of Field Robotics, 2009; 26(6-7): 537–548.

[11] Yang Y, Zhang G, Zha J Y, Li Y K, Zhang T, Chen L Q. Design of automatic steering system based on direct connection of DC motor and full hydraulic steering gear. Transactions of CSA, 2020; 51(8): 44–54, 61. (in Chinese)

[12] Wu D, Zhang Q, Reid J. Adaptive steering controller using a Kalman estimator for wheel-type agricultural tractors. Robotica, 2001; 19(5): 527–533.

[13] Ding Y, Wang L, Li Y W, Li D L. Model predictive control and its application in agriculture: a review. Computers and Electronics in Agriculture, 2018, 151: 104–117.

[14] Brewer D E. Vehicle gyro based steering assembly angle and angular rate sensor. CA 20070088477.

[15] Yin X, Du J, Noguchi N, Yang T X, Jin C Q. Development of autonomous navigation system for rice transplanter. Int J Agri & Biol Eng, 2018; 11(6): 89–94.

[16] Han H Z, Wang J, Du M Y. GPS/BDS/INS tightly coupled integration accuracy improvement using an improved adaptive interacting multiple model with classified measurement update. Chinese Journal of Aeronautics, 2018; 31(3): 556–566.

[17] Chen Y, He Y. Development of agricultural machinery steering wheel angle measuring system based on GNSS attitude and motor encoder. Transactions of CSAE, 2021; 37(10): 10–17. (in Chinese)

[18] Chen Q J, Niu X J, Kuang J, Liu J N. IMU Mounting angle calibration for pipeline surveying apparatus. IEEE Transactions on Instrumentation and Measurement, 2020; 69(4): 1765–1774.

[19] Miao C X, Chu H X, Sun Z H, Xu J Y, Ma F. Wheel turning angle measurement system based on double GNSS antennas and single gyro. Transactions of CSAM, 2017; 48(9): 17–23. (in Chinese)

[20] Miao C X, Chu H X, Cao J J, Sun Z H, Yi R R. Steering angle adaptive estimation system based on GNSS and MEMS gyro. Computers and Electronics in Agriculture, 2018; 153: 196–201.

[21] Si J Q, Niu Y X, Lu J Z, Zhang H. High-precision estimation of steering angle of agricultural tractors using GPS and low-accuracy MEMS. IEEE Transactions on Vehicular Technology, 2019; 68(12): 11738–11745.

[22] Xing H F< Hou B, Lin Z H, Guo M F. Modeling and compensation of random drift of MEMS gyroscopes based on least squares support vector machine optimized by chaotic particle swarm optimization. Sensors, 2017; 17(10): 2335–2350.

[23] Xu Q M. The research of GNSS dual-antenna/MIMU integrated algorithm. Master dissertation. Nanjing: Southeast University, 2019; 75p. (in Chinese)

[24] Cui J, Zhao Q C. Bias thermal stability improvement of MEMS gyroscope with quadrature motion correction and temperature self-sensing compensation. Micro & Nano Letters, 2020; 15(4): 234–238.

[25] Xu Q, Xiao D B, Hou Z Q, Zhou M, Li W Y, Xu X M, et al. A novel high-sensitivity butterfly gyroscope driven by horizontal driving force. IEEE Sensors Journal, 2019; 19(6): 2064–2071.

[26] Guo X T, Sun C K, Wang P, Huang L. Hybrid methods for MEMS gyro signal noise reduction with fast convergence rate and small steady-state error. Sensors & Actuators: A: Physical, 2018; 269: 145–159.

[27] Fu J, Han H X. Modified adaptive real-time filtering algorithm for MEMS gyroscope random noise. Acta Photonica Sinica, 2019; 48(12): 183–191. (in Chinese)

[28] Gautam D, Lucieer A, Watson C, McCoull C. Lever-arm and boresight

correction, and field of view determination of a spectroradiometer mounted on an unmanned aircraft system. ISPRS Journal of Photogrammetry and Remote Sensing, 2019; 155: 25–36.

[29] Sotelo M A. Lateral control strategy for autonomous steering of Ackerman-like vehicles. Robotics and Autonomous Systems, 2003; 45: 223–233.

[30] Huang X P, Mao J M. Analytical design on steering motion of wheeled vehicle. Journal of Nanjing Forestry University (Natural Science Edition), 2002; 6: 49–53. (in Chinese)

[31] Li L M, Zhao L Y, Tang X H, He W, Li F R. A compensation algorithm of gyroscope error based on modified Kalman filter. Chinese Journal of Sensors and Actuators, 2018; 31(4): 538–544. (in Chinese)

[32] Wang Q, Yang C S, Wu S E, Wang Y X. Lever arm compensation of autonomous underwater vehicle for fast transfer alignment. Computers, Materials & Continua, 2019; 59(1): 105–118.

[33] Fu Q W, Li S H, Liu Y, Zhou Q, Wu F. Automatic estimation of dynamic lever arms for a position and orientation system. Sensors (Basel, Switzerland), 2018; 18(12): 4230. doi: 10.3390/s18124230.

[34] He J, Gao W W, Wang H, Yue B B, Zhang F, Zhang Z G. Steering wheel angle measurement method of agricultural machinery based on dual MEMS gyroscope. Journal of Chinese Agricultural Mechanization, 2020; 41(4): 123–129. (in Chinese)

[35] He J, Gao W W, Wang H, Yue B B, Zhang F, Zhang Z G. Wheel steering angle measurement method based on GNSS heading differential and MEMS gyroscope. Journal of South China Agricultural University, 2020; 41(5): 91–98. (in Chinese)